Published in final edited form as:
Biofabrication. 2013 December ; 5(4): 045007. doi:10.1088/1758-5082/5/4/045007.

Biofabrication and testing of a fully cellular nerve graft

Christopher M Owens[1], **Francoise Marga**[1], **Gabor Forgacs**[1,2,3], and **Cheryl M Heesch**[2,4]

[1]Department of Physics and Astronomy, University of Missouri, Columbia MO 65211, USA

[2]Dalton Cardiovascular Research Center, University of Missouri, Columbia MO 65211, USA

[3]Department of Bioengineering, University of Missouri, Columbia MO 65211, USA

[4]Department of Biomedical Sciences, University of Missouri, Columbia MO 65211, USA

Abstract

Rupture of a nerve is a debilitating injury with devastating consequences for the individual's quality of life. The gold standard of repair is the use of an autologous graft to bridge the severed nerve ends. Such repair however involves risks due to secondary surgery at the donor site and may result in morbidity and infection. Thus the clinical approach to repair often involves non-cellular solutions, grafts composed of synthetic or natural materials. Here we report on a novel approach to biofabricate fully biological grafts composed exclusively of cells and cell secreted material. To reproducibly and reliably build such grafts of composite geometry we use bioprinting. We test our grafts in a rat sciatic nerve injury model for both motor and sensory function. In particular we compare the regenerative capacity of the biofabricated grafts with that of autologous grafts and grafts made of hollow collagen tubes by measuring the compound action potential (for motor function) and the change in mean arterial blood pressure as consequence of electrically eliciting the somatic pressor reflex. Our results provide evidence that bioprinting is a promising approach to nerve graft fabrication and as a consequence to nerve regeneration.

Keywords

cellular nerve graft; bioprinting; electrophysiology; compound muscle action potential; sensory function

1. Introduction

When a nerve is damaged or severed, the axons distal to the damaged site degenerate and must be re-enervated through the body's natural repair mechanism [1]. If the ends of the nerve can be reconnected without too much tension, the damage can be best repaired by suturing the two ends [2]. However, if this is not possible, a nerve guide is required to bridge the gap between the proximal and distal ends (respectively, still connected and not anymore connected to the cell body) to accomplish proper regrowth of axons and a progressive return of motor and sensory function [3].

An ideal nerve guide must satisfy a number of conditions to support the regrowth of axons. The graft must be biocompatible and provide a path for the growing axons to reach the distal part of the motor nerve. Immune response to the graft should be negligible, or should be

suppressed to minimize the risk of rejection [4]. The graft should be able to accommodate neurotrophic factors, such as nerve growth factors that have been shown to improve regeneration when added to the conduit directly, or indirectly produced through seeding the nerve conduit with Schwann cells (SC), the major cell type that supports neurons in the peripheral nervous system [4–6].

Currently, the gold standard for nerve repair requiring a conduit is an autograft (a nerve segment transplanted from another part of the individual to the damaged site). However, there are a number of pitfalls to using an autograft, including matching the diameter and mechanical properties of the nerve [7], risking morbidity to the donor site, and the overall risk of multiple surgeries [2]. Autografts are typically derived from sensory nerves, leading to suboptimal regeneration in the case of motor nerve damage. Another common approach is to use vein tissue as autograft [8]. These show good functional repair in clinical applications for small gaps [9], especially when combined with muscle tissue [8] or nerve slices [9]. In the absence of autografts, allografts (a nerve segment transplanted from a genetically non-identical donor of the same species) have been used with satisfactory outcome, but they require immunosuppression therapy to avoid rejection [2, 10].

Because of these challenges when using donor tissue, a number of engineering approaches have been proposed [3, 11, 12]. Synthetic materials such as silicone, polytetrafluoroethylene, polypropylene, and others [13, 14] have been used in clinical trials [15], but did not show good recovery in nerve defects over 4 cm [16]. Grafts have also been made from fibrous composites [11] and/or extracellular matrix (ECM) materials, such as collagen [11, 17, 18], laminin [19] and fibronectin [20]. In a number of studies with synthetic or ECM material-based grafts Schwann cells or growth factors were added. These studies showed that conduits seeded with Schwann cells, in general, perform better [21–24]. This was true even when synthetic components to mimic Schwann cells were added [25].

Collagen tubes have been particularly noted for their regenerative capability, and have been approved for clinical uses in humans [26]. In extended animal trials with primates, the collagen nerve guide showed comparable levels of motor response when compared to direct suture and autografting after 12 weeks [27]. In some clinical studies, up to 89% of the patients receiving the collagen graft regained good function to the affected area [28, 29]. The wide use of this graft makes it also a useful second control for testing the quality of experimental grafts [30]. While these approaches have had considerable success, they are still outperformed by autologous grafts, which when available, remain the surgeon’s first choice.

We developed a technology to biofabricate a purely cellular nerve graft, with properties potentially analogous to those of an autologous graft, but free of the risks associated with the latter. We employed bioprinting [31–33] to fabricate the fully biocompatible conduit using mouse bone marrow stem cells (BMSC) and SC. To evaluate the functionality of this novel type of nerve graft we have optimized it for study in a rat sciatic nerve injury model [31]).

Our bioprinted grafts have several advantages over other types of engineered nerve conduits. The fully cellular approach matches more closely the gold standard of using an autograft

than other synthetic and biocompatible conduits. Ideally, these constructs would be made with cells cultured from the individual in need of the transplant, preventing the rejection by the immune system. As mentioned, sizing can be an issue with autografts. The bioprinting process allows for the exact dimensions required for the needed graft, without relying on finding the properly sized nerve or preconstructed tube. Bioprinting also assures that modifications to the graft can easily be incorporated (e.g. using different types of cells, adding extra growth factors), thus to possibly supersede the capabilities of an autograft.

In ref. [31] we described the fabrication of our nerve graft as well as its implantation, with limited data on nerve regeneration. We reported on axonal regrowth three weeks post-implantation. Physiological testing was not included in this previous study, and there was no comparison to other standards of repair. Here, we report on the comparison between our biofabricated construct and two benchmarks for nerve repair: collagen tube and autograft. We carried out functional analysis by measurements of the compound muscle action potential (CMAP). CMAP represents the summary simultaneous response of several muscle fibers from the same area of the body evoked by the electrical stimulation of a motor nerve. We have also measured sensory responses evaluated by the increase in blood pressure in response to eliciting the somatic pressor reflex (SPR) by electrical stimulation of the same nerve. Finally, we evaluated axon growth through the grafts by histological investigation. Our objective with the present study is to demonstrate that bioprinting represents a promising approach to build architecturally complex conduits for superior nerve repair. In particular, we show that even the geometrically relatively simple conduits we have so far fabricated compare favorably with standard clinical methods presently employed.

2. Materials and Methods

2.1 Cell culture and preparation of the multicellular cylinders

For the fabrication of the engineered nerve grafts by bioprinting we used “bioink” particles [32, 33], multicellular cylindrical units with composing cells, such as BMSC and SC known to favor nerve regeneration. Their preparation was detailed elsewhere [31]. In brief, the BMSC cells (kindly acknowledged gift from Roger Markwald, Medical University of South Carolina, Charleston, SC) were cultured in IMDM (Gibco, Life Technologies, Green Island, New York) supplemented with 12% FBS, 12% DES (Thermo Fisher, Waltham, Massachusetts), 0.1mg/ml Penicillin/Streptomycin (Gibco, Life Technologies, Green Island, New York) and 1 macromolar Hydrocortisone (Sigma-Aldrich, St. Louis, MO). The SC (ATCC, Manassas, VA) were cultured in DMEM (Gibco, Life Technologies, Green Island, New York) supplemented with 10% FBS and 0.1mg/ml Pen-Strep. During subculture the cells were washed twice with Phosphate Buffered Saline (Gibco, Life Technologies, Green Island, New York), and detached using a 0.1% Trypsin EDTA solution (Gibco, Life Technologies, Green Island, New York) then centrifuged at 1.5g (2000 RPM) for 5 minutes. The supernatant was removed and the cell pellet was resuspended in 2 mL of medium per culture dish for the BMSC, and 4 mL for SC (the latter grow much faster). 1 mL of the cell suspension was dispensed over 7 mL of the cell’s medium in a 10 cm diameter tissue culture dish (TPP, Trasadingen, Switzerland).

To prepare the pure BMSC cylinders, the cell pellet from 4 dishes was instead resuspended in 400 μL of medium in a 2 mL Eppendorf microcentrifuge tube, inside of a 15 mL centrifuge tube. This was spun down at about 5g (5000 RPM) for two minutes. The supernatant was removed, and the cell pellet was aspirated into 0.5 mm inner diameter capillary tubes, which were subsequently incubated in medium for about 15 minutes to form the cellular cylinders. Note that the cell density of in the cellular cylinders by construction is maximal. The cellular cylinders were then extruded into customized agarose molded wells (see ref. [32, 33]) containing medium and incubated for ~4 h. For the mixed SC and BMSC cylinders, the two cell suspensions were mixed and densities adjusted to arrive at 90%BMSC/10% SC mixture. This mixture was then used to prepare cellular cylinders as described above.

2.2 Design and construction of the conduit

Details of the biofabrication method we employed to build the biological nerve conduit have been described elsewhere [31]. In brief, using a bioprinter, the discrete ~500 micron diameter cellular cylinders were deposited into a support structure according to a specific design template [31] compatible with the overall geometrical properties of a multi-luminal graft to be used in a rat sciatic nerve injury model (~1 cm length, ~2 mm diameter). Multi-luminal channels were incorporated in the design to potentially facilitate axon regrowth. We chose ~500 micron diameter cellular cylinders, as this is the classic dimension in our bioprinting process (we have used others [31]). This size in general assures minimal cell death in the interior of the cylinder, as nutrients from the culture medium can reach more or less every cell by diffusing not more than 250 microns. In the case of the nerve graft in particular the 500 micron diameter was suggested in [24], where this channel diameter in a multi-luminal nerve graft gave the best result. The biological graft formed post-printing, by the fusion of the bioink cylinders. Once fusion was complete the external support, made of agarose, impermeable to cells, was removed. After a maturation period of seven days, the multichannel construct developed sufficient mechanical integrity to be implanted into a laboratory rat. The design template and the triple-lumen final graft are shown in figure 1.

2.3 Implantation

Using aseptic technique, Female Sprague-Dawley rats were used to surgically isolate and remove a 1 cm section of their sciatic nerve [31]. The resulting gap was bridged with either an autologous graft (nerve section excised, rotated 180 degrees, and sutured back into the rat), a commercial hollow collagen nerve guide, widely used in comparative studies [30, 34] as well as in clinical settings [28, 29, 35] (NeuraGen, Integra Life Sciences, Plainboro, NJ) or the biofabricated nerve tube. To secure the engineered nerve tube it was floated into a longitudinally cut collagen nerve guide, approximately 12 to 14 millimeters in length. The wound was then irrigated, the muscle and skin closed. Animals were allowed to recover and experiments were performed approximately 40 weeks later. All animal protocols were approved by the University of Missouri Animal Care and Use Committee and were in compliance with the National Institutes of Health “Guide for the Care and Use of Laboratory Animals.”

2.4 Electrophysiological study: evaluation of motor function recovery

In these studies, initially, ten rats were prepared for stimulation of the sciatic nerves and recording of the compound muscle action potentials (CMAP). Depending on how the excised nerve section was bridged, animals were classified into three groups: autologous graft (3 rats), collagen tube graft (3), and biofabricated graft (4). As these are pilot experiments to evaluate long term functional recovery there is always concern of technical difficulties and therefore we started with one more animal in the biofabricated construct group (our major interest). Anesthesia was induced with isoflurane (5%; Baxter, Deerfield, IL) and maintained with inactin (100 mg/kg, i.v.; Sigma-Aldrich, St. Louis, MO); the trachea was cannulated and catheters were implanted in the inferior vena cava and carotid artery for administration of drugs and measurement of arterial blood pressure respectively. The sciatic nerve was isolated and a bipolar stainless steel hook electrode was placed as close to the sciatic notch as possible, proximal to the nerve graft. (Stimulating electrode placement was anatomically similar on the unrepaired sciatic nerve in the control leg). Bipolar prong stainless steel recording electrodes were placed in the middle of the gastrocnemius muscle and secured with a suture. A ground wire was placed nearby, distal to the site of recording. Technical difficulties prevented placement of the stimulating electrode proximal to the site of nerve repair in one of the rats in the biofabricated graft group and this rat was removed from the study. Another rat in the same group had a uterine infection, and was also excluded from the study. The mean weight of the eight remaining rats at the time of the study was 317 ± 9 g.

The sciatic nerve proximal to the graft was placed on the stimulating electrode and biphasic 0.1 ms pulses, at a rate of 1 Hz, were applied to the nerve using a Winston A65 stimulator and two SC-100 monophasic constant current isolators (Winston Electronics Co, Milbrae, CA). The current was incrementally increased until the minimum current that reproducibly evoked a CMAP in the gastrocnemius muscle (threshold current) was reached. For each current setting, the pulse was repeated approximately 10 times, and measurements at that current were averaged for analysis (the standard deviation over the 10 measurements in each case was ± 0.05 for all the values shown in Table 1). These measurements were performed for both the experimental leg (nerve repair), and the control (unoperated) leg for each of the rats, for comparison. The CMAP was recorded using a Grass P511 amplifier and high impedance probe (HIP511E; Grass Instruments, Quincy, MA). Data were first collected for the rat's experimental leg, and then from that rat's control leg. Comparison of responses at 5 times and 10 times threshold current were similar, and thus 5X threshold was considered maximally effective and these data were used for statistical comparisons.

2.5 Electrophysiological study: evaluation of sensory function recovery

To evaluate sensory function, we elicited the somatic pressor reflex (SPR), a cardiovascular response to activation of muscle sensory nerves [36], by electrically stimulating the sciatic bundle distal to the graft and measuring the resultant reflex as an increase in mean arterial pressure (MAP). The rat was artificially ventilated and paralyzed with a neuromuscular blocker, gallamine triethiodide (25mg/kg/hr, i.v. infusion, Sigma-Aldrich, St. Louis, MO). The stimulating electrode was repositioned to a site distal to the graft. Using a Grass S48 stimulator and PSIU6 constant current stimulation unit (Grass Instruments, Quincy, MA) a

20 Hz, 1 ms square wave stimulus was applied. A cumulative stimulus-pressure relationship was determined by gradually increasing stimulus current from 0.1 mA to 1.5 mA. Increments of 0.05 mA were used for the first 0.4 mA, and then 0.1 mA increases after that.

Following recordings of the CMAP on the experimental and then the control leg, the above preparations were made, and the SPR was evaluated in the control leg, followed by the experimental leg.

Data were acquired and analyzed using PowerLab Data Acquisition System and LabChart 7 software (AdInstruments, Colorado Springs, CO). Mean arterial pressure (MAP) was calculated on-line from pulsatile arterial pressure (MAP = 1/3 systolic + 2/3 diastolic pressure) and displayed continuously on a separate channel. Measurements of latency and MAP were performed off-line.

2.6 Statistical analysis

Statistical analysis was performed with two-way ANOVA for repeated measures using SigmaPlot 12 (Systat Software, Chicago IL). The two factors compared were Group (implant graft: autologous, collagen tube, biofabricated) and Treatment (control leg vs. experimental leg). The two-way ANOVA was performed for the latency to peak data and the maximum blood pressure response during the sensory pressor reflex. A one-way ANOVA was also performed for the ratios (repair/control) of the aforementioned data.

2.7 Evaluation of axon regrowth

After the electrophysiology experiments, grafts were harvested (using a surgical procedure similar to the one for implantation) with the proximal and distal nerve stumps and photographed for morphological observations. Tissues were fixed (overnight in 4% paraformaldehyde) and prepared for histological assessments (i.e. dehydrated with an ethanol series, sectioned and processed for paraffin infiltration and embedding). Bielschowsky's Silver Staining [37, 38] was used to visualize axons in histological sections along the repair, near the middle of the graft, using high magnification (200x) photographs of the sections, acquired with a Nikon Eclipse 6600 microscope (Nikon Inc, Melville, NY) equipped with an Olympus DP72 camera using DP2 BSW software (Olympus, Center Valley, PA). Additional photographs were taken in select areas at 600x magnification to obtain more detailed visualizations of some of the areas of the graft.

3. Results

3.1 Electrophysiology: Compound Muscle Action Potential

A CMAP measurement consists of recording voltage changes in the muscle as a function of time in response to electrical stimulation of the innervating nerve. Typical measurements of interest include [39]: latency to response (the time delay between nerve stimulation to the beginning of a detectable response in the muscle) and latency to peak response (the time delay between nerve stimulation and the point of maximum amplitude of the CMAP). These quantities (see figure 2) characterize distinct properties of nerve conduction. Latency correlates with the speed of conductance, with latency to response involving only the fastest

axons, whereas latency to peak represents the conduction along the majority of axons. Because of the variability in size and duration of the stimulus artifact (figure 2) among rats, and possible inaccuracy in determining the beginning of the muscle response, we used the data for latency to peak response [40] (figure 2) to compare the CMAP across the three types of grafts (autologous, collagen tube, biofabricated).

In table 1 and figure 3 we quantitatively compare the latency to peak data across the three groups of grafts. Table 1 contains the numerical values of latency to peak for all rats. As expected, the latencies typically decreased with increasing current, and were longer in the repaired than in the control legs. It is also expected that with increasing current the latency of the repaired leg for each graft should approach the latency of the control leg. Indeed, a two way ANOVA showed a significant difference of overall treatment (control leg vs. repair leg) at threshold for the biofabricated and collagen tube grafts. This difference disappeared at 5x for the biofabricated graft, but was still present for the collagen tube (it remained present at all levels of stimulation), hinting that our construct may have superior repair to the collagen tube, regarding latency. Finally, we found no significant difference between control and the autologous graft at any level of stimulation.

In figure 3 this comparison is shown in terms of the ratio of the peak latencies in the repaired versus control legs. Such representation of the data takes into account the inevitable variation between individual animals. A ratio of 1.0 would represent complete recovery of function. The ratios shown in figure 3 are comparable to those of other bipolar stimulation studies using various nerve guides and measurement of CMAP in the gastrocnemius muscle [13]. The limited data set in figure 3 suggests that (not surprisingly) the autologous graft might perform the best among the three and the biofabricated graft may be superior to the pure collagen tube graft.

3.2 Electrophysiology: Sensory Response

Recovery of sensory function in the sciatic nerve repair model was evaluated by measuring the increase in MAP in response to afferent stimulation of the sciatic nerve (somatic pressor reflex) for both the control and the experimental leg. The stimulating electrode was positioned on the nerve distal to the repair site (in the operated leg) and baseline blood pressure (prior to electrical stimulation) was noted. (Electrode placement was at an anatomically similar site on the control leg.) MAP was continuously recorded as 1 ms square wave pulses (20 Hz), at progressively increasing currents, were applied to the nerve to elicit the somatic pressor reflex (figure 4). Off-line analysis included measurement of baseline MAP and the maximum MAP achieved during sciatic nerve stimulation (a stable region of ~ 3 to 5 seconds of data was electronically averaged as indicated by the dashed-line boxes in the example shown in figure 4). MAP was recorded when the response reached a plateau between increases in current, or was averaged for the region between current changes if no plateau occurred (figure 4). Maximum blood pressure was obtained by noting the highest blood pressure achieved in the data set (figure 4). MAP values for individual rats in the three groups are provided in table 2.

In figure 5 data is expressed as the ratio of the maximum blood pressure achieved with the SPR elicited from the repaired versus control sciatic nerve. Such representation of the data

takes into account the inevitable variation between individual animals. Although it appeared that the stimulus response curve was shifted toward higher stimulation currents across the repaired nerve (Figure 4), the maximum blood pressure response was similar to that obtained by stimulation of the unoperated nerve (figure 5, ratio near 1.0). This was reinforced by a two-way ANOVA, which showed no difference between baseline blood pressure, maximum blood pressure, and the change in blood pressure among the three groups.

3.3 Axon regrowth

Once the various grafts were excised, we prepared histological sections, taken at mid graft, on which we performed Bielschowsky's staining [37, 38] to visualize axons, as a standard metric of repair. First, we attempted to define an axon density across the graft's cross-section. As the biofabricated grafts contained multiple lumina the distribution of axons across the graft's cross section was highly inhomogeneous, which made the use of an axon density as a means of comparison unreliable. However, a qualitative comparison of the axons across the grafts was still possible as shown in figure 6. The figure displays reasonable axon regrowth across all of the groups. It is important to note that in the biofabricated graft there is a higher density of axons near the lumina of the tissue (figure 6E), where the Schwann cells are located (see figure 1). In the trials presented here, the agarose rods within the construct were not removed prior to surgical implantation (see figure 1F). It appears that the presence of agarose within the channel prevented regrowth, as there were no visible axons through these agarose-containing regions of the construct (figure 6B and 6E). These results together with data on axon counts, in our earlier work (see figure 8 in ref. [31] at both the proximal and distal ends of the conduit) and the electrophysiological measurements as reported here, provide convincing evidence that extensive axonal regrowth has taken place across the biofabricated grafts.

4. Discussion and future work

This study describes the testing of a nerve graft fabricated by using bioprinting, to our knowledge, for the first time. An additional novelty of our graft is that it can be prepared as a fully cellular construct whereas most other approaches use synthetic or ECM-based conduits, which either are or are not seeded with cells [42]. (We are aware of only one work reporting on the fabrication of a fully cellular graft, albeit using an approach substantially different from ours [43].) Furthermore, due to the flexibility of the fabrication method, the bioprinted grafts can easily be modified and improved, as discussed below.

The multi-luminal graft was prepared using a combination of cylindrical bioink particles composed of BMSC, SC and agarose. The graft was reinforced with a surrounding collagen tube. In our earlier work [31] with short-term post-implantation studies the presence or removal of the agarose rods did not seem to affect the graft's functionality. Thus in the current study, for convenience, the agarose rods in the construct's interior were not removed. The presence of agarose does provide mechanical integrity to the graft and makes its handling (and thus the implantation) easier. It is always retained until the multicellular cylinders fuse post-printing. However, once fusion is complete and cells build their own ECM, the cellular construct gradually develops its own mechanical strength. This was

evident in our bioprinted vascular grafts prepared in a similar process as used here. Such grafts, once the agarose rod was removed from their lumen, when perfused, manifested gradually increasing burst pressures implying increasing mechanical strength [31].

Histology indicated that over the longer time (40 weeks in the present study) the presence of agarose in our nerve graft might have limited axon regrowth in those regions. However, axon regrowth was evident in regions surrounding the agarose rods. In further studies, it will be of high priority to remove the agarose rods. (We refer to our graft as potentially fully cellular because, as demonstrated, it can be fabricated without agarose, which is the only non-cellular material.)

BMSCs were chosen for two reasons. First, the graft could not be composed solely of SC, as these cells (as opposed to BMSCs) only weakly adhere to each other. Therefore fusion of the multicellular cylinders composed of only these cells does not result in sufficient mechanical integrity. (The tendency of Schwann cells to form sheets to cover axons does not favor the fusion of the cylinders.) Secondly, in addition to the higher affinity of BMSCs to one another, they can be isolated and differentiated into SC, and are compatible with nerve regeneration [16.1 21, 29.1 44]. This latter property is a distinguishing feature of our graft and may play an important role in the mechanism of regeneration. As shown in ref. [29.1] BMSCs can efficiently be induced to differentiate into cells with Schwann cell properties. In our grafts such differentiation might be triggered by factors secreted by the native Schwann cells. Upon transplantation such a mechanism could provide an additional source of Schwann cells “as needed”.

Through electrophysiological testing we compared our construct with two standard methods of nerve repair, the autologous graft and the collagen tube grafts. We have shown functional efferent (i.e. motor) nerve repair by testing the CMAP and afferent (i.e. sensory) repair by eliciting the somatic pressure reflex in all of the groups. Other studies evaluating recovery following nerve repair in rats typically evaluated motor recovery only and have been performed within 12 weeks of repair [45–47]. In the current experiments, we demonstrate recovery of both motor and sensory function, and found that each graft performed satisfactorily when tested after an extended period of time following repair (40 weeks). As the compared controls are known to consistently provide good repair [2, 28], and our construct performed at a similar level (if not better than the collagen tube), these experiments affirm the long term functionality of our biofabricated nerve graft.

As ours is a bioprinted nerve conduit, which can be fabricated from exclusively cellular components, and as such differs considerably from earlier engineered grafts, it is useful to compare its functional properties with earlier reports on synthetic and ECM-based grafts in the rat sciatic nerve model. Such comparison however is limited by the fact that details for stimulation parameters are often not provided. Several reports using techniques most similar to ours (bipolar nerve electrodes, responses to increasing stimulation current) used stimulus durations between 50 and 200 microseconds [48–51]. Therefore our choice of 100 microseconds (0.1 ms) was consistent with previous studies. The most important feature of these types of experiments is to verify that supramaximal stimuli are applied and this was

the case with 5X threshold currents. The use of biphasic square wave stimuli to the nerve is commonly used to reduce stimulus artifact in the CMAP recording.

Carmen and Vlegger-Lankamp [13] provide an exhaustive review on the properties of bioengineered grafts in rat sciatic nerve models (until 2004). Table 10 in that reference contains the data on latency. Results for experiments most closely comparable to ours and expressed in terms of the ratio of the latency on the experimental side to the latency on the contralateral, untreated side vary in the range 1.1–1.45 and 1.3–4.5, respectively, for the autologous and synthetic or ECM-based grafts. These ratios compare favorably with our results that can be derived from Table 1 in this work, which are 1.1–1.3, 1.2–1.4, 1.1–1.8, respectively, for the autologous, bioprinted and collagen tube grafts. (Even though these numbers were obtained from data at 5X threshold for data on latency to peak, given that they represent ratios, we believe the comparison with published results in ref. [13] is meaningful, representative and useful.)

In order to provide a more statistically significant study, we plan to modify the *in vitro* method of Vyas et al [52] to further test the repair capabilities of the biofabricated grafts. An in vitro study of nerve repair allows for a much larger sample size than our current study presented. In addition, such a study can be carried out on a shorter time scale (1–2 weeks), allowing for the testing of a variety of constructs to arrive at the optimal one, before proceeding to the considerably more complex studies performed on live animals.

5. Conclusions

In conclusion, while our sample size is small to provide definitive evidence whether or not our construct performed better than the standard collagen tube, our results are encouraging and suggest that this might be the case. It should be stressed that the objective of the present work was to develop a proof-of-concept for a new type of nerve graft and its functional testing, which we have shown. As this is a first attempt to biofabricate a fully cellular bioprinted nerve graft, there are many adjustments that will need to be made to improve and eventually optimize the performance of such a graft. Removing the agarose rods from the construct lumina prior to implantation or using a hydrogel with faster degradation time *in vivo*, adjusting the number of lumina [24, 30], modifying the cell types used or adding growth factors are some of the possibilities that could further improve nerve repair.

Acknowledgments

The authors acknowledge the expert technical assistance of Mr. J. Glenn Phaup in the conduct of *in vivo* physiological experiments. Christopher Owens, Francoise Marga and Gabor Forgacs acknowledge the partial support of NSF under grant EF0256854, as well as the support of the University of Missouri Research Foundation. Cheryl Heesch acknowledges partial support by NIH HL091164.

References

1. Fawcett JW, Keynes RJ. Peripheral nerve regeneration. Annu Rev Neurosci. 1990; 13:43–60. [PubMed: 2183684]
2. Siemionow M, Brzeziki G. Current techniques and concepts in peripheral nerve repair. Int Rev Neurobiol. 2009; 87:141–72. [PubMed: 19682637]

3. Schmidt CE, Leach JB. Neural tissue engineering: strategies for repair and regeneration. Annu Rev Biomed Eng. 2003; 5:293–347. [PubMed: 14527315]
4. Ruiter, GCWd, et al. Designing ideal conduits for peripheral nerve repair. Neurosurg Focus. 2009; 26:E5. [PubMed: 19435445]
5. Subramanian A, Krishnan UM, Sethuraman S. Development of biomaterial scaffold for nerve tissue engineering: biomaterial mediated neural regeneration. J Biomed Sci. 2009; 16:108. [PubMed: 19939265]
6. Hood B, Levene HB, Levi AD. Transplantation of autologous Schwann cells for the repair of segmental peripheral nerve defects. Neurosurg Focus. 2009; 26:E4. [PubMed: 19435444]
7. Wolford LM, Stevao ELL. Considerations in nerve repair. Proc (Bayl Univ Med Cent). 2003; 16:152–6. [PubMed: 16278731]
8. Battiston B, et al. Nerve repair by means of vein filled with muscle grafts: I clinical results. Microsurgery. 2000; 20:32–6. [PubMed: 10617879]
9. Tang JB, Gu YQ, Song YS. Repair of digital nerve defect with autogeneous vein graft during flexor tendon surgery in zone 2. J Hand Surg Br. 1993; 18:449–53. [PubMed: 8409654]
10. Moore AM, et al. Nerve allotransplantation as it pertains to composite tissue transplantation. Hand. 2009; 4:239–44. [PubMed: 19306048]
11. Daily W, Yao L, Zeugolis D, Winderbank A, Pandit A. A biomaterials approach to peripheral nerve regeneration: bridging the peripheral nerve gap and enhancing functional recovery. J R Soc Interface. 2012; 9:202–21. [PubMed: 22090283]
12. Clements IP, et al. Regenerative scaffold electrodes for peripheral nerve interfacing. IEEE Trans Neural Syst Rehabil Eng. 2013; 21:554–66. [PubMed: 23033438]
13. Carmen LAM, Vleggeert-Lankamp MD. The role of evaluation methods in the assessment of peripheral nerve regeneration through synthetic conduits: a systematic review. J Neurosurg. 2007; 107:1168–89. [PubMed: 18077955]
14. Belkas JS, Shoichet MS, Midha R. Peripheral nerve regeneration through guidance. Neurol Res. 2004; 26:151–60. [PubMed: 15072634]
15. Schlosshauer B, et al. Synthetic nerve guide implants in humans: a comprehensive survey. Neurosurg. 2006; 59:740–8.
16. Stanec S, Stanec Z. Reconstruction of upper-extremity peripheral-nerve injuries with ePTFE conduits. J Reconstr Microsurg. 1998; 14:227–32. [PubMed: 9618088]
17. Yoshii S, et al. 30 mm regeneration of rat sciatic nerve along collagen filaments. Brain Res. 2002; 949:202–8. [PubMed: 12213317]
18. Ceballos D, et al. Magnetically aligned collagen gel filling a collagen nerve guide improves peripheral nerve regeneration. Exp Neurol. 1999; 158:290–300. [PubMed: 10415137]
19. Kauppila T, et al. A laminin graft replaces neurrorhaphy in the restorative surgery of the rat sciatic nerve. Exp Neurol. 1993; 123:181–91. [PubMed: 8405284]
20. Ahmed Z, ABR. Adhesion, alignment, and migration of cultured Schwann cells on ultrathin fibronectin. Biomaterials. 1999; 21:1541–47.
21. Rodrigues MCO, et al. Peripheral nerve repair with cultured Schwann cells: getting closer to the clinics. Scientific World Journal. 2012; 2012:413091. [PubMed: 22701355]
22. Udina, Esther, et al. FK506 enhances regeneration of axons across long peripheral nerve gaps repaired with collagen guides seeded with allogenic Schwann cells. Glia. 2004; 47:120–9. [PubMed: 15185391]
23. Madduri S, Gander B. Schwann cell delivery of neurtrophic factors for peripheral nerve regeneration. J Peripher Nerv Syst. 2010; 53:93–103. [PubMed: 20626772]
24. Hadlock T, Sundback C, Hunter D, Cheney M, Vacanti JP. A polymer foam conduit seeded with Schwann cells promotes guided peripheral nerve regeneration. Tissue Eng. 2000; 6:119–27. [PubMed: 10941207]
25. Lee J-Y, et al. The effect of collagen nerve conduits filled collagen-glycosaminoglycan matrix on peripheral motor nerve regeneration in a rat model. J Bone Joint Surg Am. 2012; 94:2084–91. [PubMed: 23172326]

26. Meek MF, Coert JH. US Food and Drug Administration/Conformit Europe-approved absorbable nerve conduits for clinical repair of peripheral and cranial nerves. Ann Plast Surg. 2008; 60:110–6. [PubMed: 18281807]
27. Archibald SJ, et al. A collagen-based nerve guide conduit for peripheral nerve repair: an electrophysiological study of nerve regeneration in rodents and nonhuman primates. J Comp Neurol. 1991; 306:685–96. [PubMed: 2071700]
28. Wangensteen KJ, Kalliainen LK. Collagen tube conduits in peripheral nerve repair: a retrospective analysis. Hand. 2010; 5:273–77. [PubMed: 19937145]
29. Taras JS, et al. Reconstruction of digital nerves with collagen conduits. J Hand Surg Am. 2011; 36:1441–6. [PubMed: 21816545]
30. Yao L, et al. Controlling dispersion of axonal regeneration using a multichannel collagen nerve conduit. Biomaterials. 2010; 31:5789–97. [PubMed: 20430432]
31. Marga F, et al. Toward engineering functional organ modules by additive manufacturing. Biofabrication. 2012; 4:022001. [PubMed: 22406433]
32. Jakab K, et al. Tissue engineering by self-assembly and bio-printing of living cells. Biofabrication. 2010; 2:022001. [PubMed: 20811127]
33. Norotte C, et al. Scaffold-free vascular tissue engineering using bioprinting. Biomaterials. 2009; 30:5910–7. [PubMed: 19664819]
34. Whitlock EL, et al. Processed allografts and type I collagen conduits for repair of peripheral nerve gaps. Muscle Nerve. 2009; 39:787–99. [PubMed: 19291791]
35. Farole A, Jamal BT. A bioabsorbable collagen nerve cuff (NeuraGen) for repair of lingual and inferior alveolar nerve injuries: a case series. J Oral Maxillofac Surg. 2008; 66:2058–62. [PubMed: 18848102]
36. Mitchell JH, Kaufman MP, Iwamoto GA. The exercise pressor reflex: its cardiovascular effects, afferent mechanisms, and central pathways. Annu Rev Physiol. 1983; 45:229–42. [PubMed: 6342515]
37. Bielschowsky M. Eine modifikation meines silverimprägnationsverfahrens zur darstellung der neurofibrillen. J für Psychologie Neurologie. 1908; 12:135–37.
38. Fitzgerald MJ. A general-purpose silver technique for peripheral nerve fibers in frozen sections. Stain Technol. 1963; 38:321–7. [PubMed: 14072208]
39. Mallik A, Weir AI. Nerve Conduction Studies: Essentials and Pitfalls in Practice. J Neurol Neurosurg Psychiatry. 2005; 76:ii23–ii31. [PubMed: 15961865]
40. Freeman, TL., et al. Nerve Conduction Studies (NCS). In: Cuccurullo, S., editor. Physical Medicine and Rehabilitation Board Review. New York: Demos Medical Publishing; 2004. Available from: http://www.ncbi.nlm.nih.gov/books/NBK27199/
41. Simpson JA. Fact and fallacy in measurement of conduction velocity in motor nerves. J Neurol Neurosurg Psychiat. 1964; 27:381–5. [PubMed: 14213466]
42. McGrath AM, et al. BD™ PuraMatrix™ peptide hydrogel seeded with Schwann cells for peripheral nerve regeneration. Brain Res Bull. 2010; 83:207–13. [PubMed: 20633614]
43. Baltich J, et al. Development of a scaffoldless three-dimensional engineered nerve using a nerve-fibroblast co-culture. In Vitro Cell Dev Biol Anim. 2010; 46:438–44. [PubMed: 19997868]
44. Wakao S, et al. Long-term observation of auto-cell transplantation in non-human primate reveals safety and efficiency of bone marrow stromal cell-derived Schwann cells in peripheral nerve regeneration. Exp Neurol. 2010; 223:537–47. [PubMed: 20153320]
45. Zhang P, et al. The experimental study of absorbable chitin conduit for bridgin peripheral nerve defect with nerve fasciculu in rats. Artif Cells Blood Substit Immobil Biotechnol. 2008; 36:360–71. [PubMed: 18649171]
46. Bian Y-Z, et al. Evaluation of poly(3-hydroxybutyrate-co-3-hydroxyhexanoate) conduits for peripheral nerve regeneration. Biomaterials. 2009; 30:217–25. [PubMed: 18849069]
47. Pan H-C, et al. Enhanced regeneration in injured sciatic nerve by human amniotic mesenchymal stem cell. J Clin Neurosci. 2006; 13:570–5. [PubMed: 16769515]

48. Valero-Cabre A, et al. Superior muscle reinnervation after autologous nerve graft or poly-L-lactide-e-caprolactone (PLC) tube implantation in comparison to silicone tube repair. J Neurosci Res. 2001; 63:214–23. [PubMed: 11169632]

49. Robinson PH, et al. Nerve regeneration through a two-ply biodegradable nerve guide in the rat and the influence of ACTH4-9 nerve growth factor. Microsurgery. 1991; 12:412–9. [PubMed: 1662750]

50. Evans PJ, Bain JR, Mackinnon SE, Makino AP, Hunter DA. Selective reinnervation: a comparison of recovery following microsuture and conduit nerve repair. Brain Res. 1991; 559:315–21. [PubMed: 1794104]

51. Valero-Cabre A, Navarro X. H reflex restitution and facilitation after different types of peripheral nerve injury and repair. Brain Res. 2001; 919:302–312. [PubMed: 11701142]

52. Vyas A, et al. An in vitro model of adult mammalian nerve repair. Exp Neurol. 2010; 223:112–8. [PubMed: 19464291]

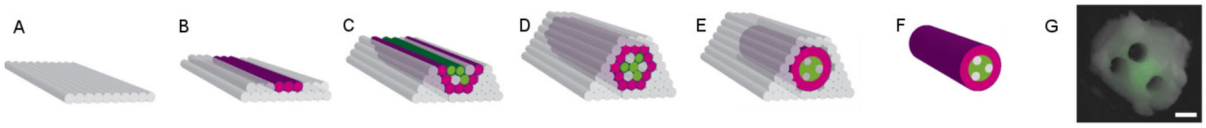

Figure 1.

Nerve graft fabrication. (A–F) show the schematic layer by layer printed structure with the types of cylinders used and their arrangement. The printed graft was made using 0.5 mm diameter multicellular cylinders. The outer ring was made of bioink units composed completely of BMSC (red). Then, cylinders comprised of 90% BMSC and 10% SC (green) were alternated with agarose rods (grey), which gave rise to multiple lumina in the interior of the graft (C–E). The structure is supported by an array of agarose rods (E), which hold the conduit in place while the discrete bioink cylinders self-assemble (i.e. fuse) into the nerve graft (F). The supporting agarose rods are removed after 7 days. Panel (G) shows the cross section of the final graft with fluorescently labeled (green) Schwann cells. Removal of the agarose rods from the fused construct resulted in three hollow channels and a fully cellular graft, as shown [31]. These channels were designed to mimic nerve fascicles upon implantation. It was originally intended to remove the lumen-forming agarose rods from each biofabricated construct before implantation. However, in this preliminary study they were left intact to provide further support to the engineered conduit. The presence of these agarose rods was found not to be critical to the functionality of the graft.

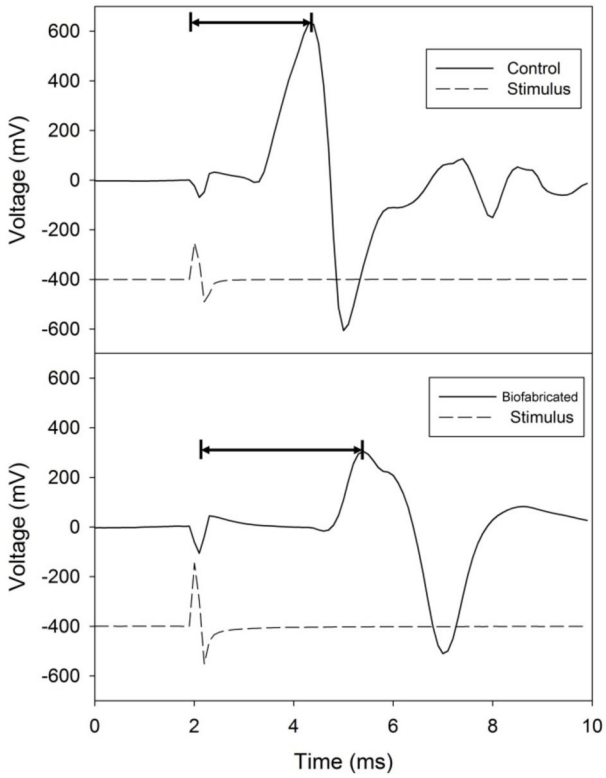

Figure 2.

Electrophysiology for motor function recovery: measurement of CMAP. The top and bottom panels are examples of evoked CMAP in the control leg (top) and the leg repaired with the biofabricated graft (bottom) from the same animal. Broken and solid lines correspond respectively to the stimulator output and the recorded CMAP. In the examples shown here, the stimulus artifact (i.e. the decay of the stimulating signal) and the response are clearly discernible in the muscle recording. However in some experiments the latency to response can be obscured by a stimulus artifact [41], as it may overlap with the start of the CMAP response, causing uncertainty in determining the beginning of the evoked response. Thus, for consistency in comparisons among animals, latency to peak response was evaluated in all rats in the current experiments, as this quantity is not affected by a stimulus artifact. Horizontal lines denote latency to peak measurement. The stimulus trace (broken line) is a recording of the stimulator output. It is provided for reference only and is not to scale.

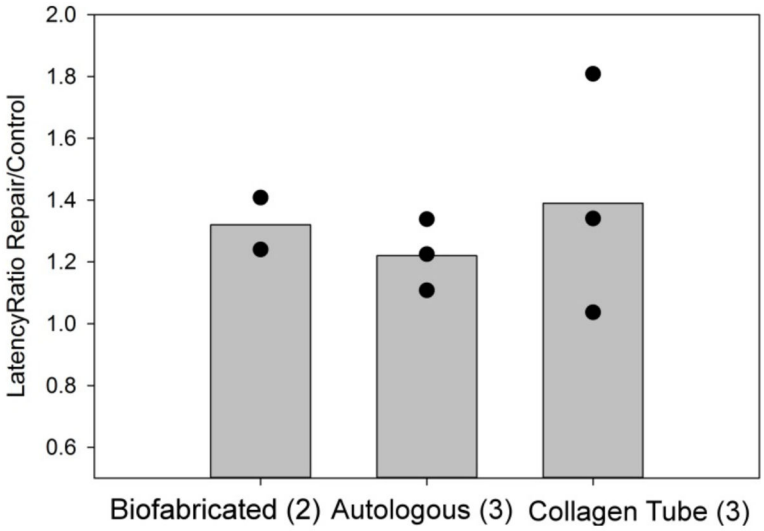

Figure 3.

Latency to peak. The bar graphs show the average values of the ratios of peak latencies measured in the repair vs. control legs in the three types of grafts. Data points indicate the ratio for individual rats in that group, whose sample size is given in parenthesis. Given that the collagen tube grafts were obtained from commercial sources, thus were identical in each animal, the relatively larger spread of data in this group could be the consequence of the larger variation among the animals in this group. However, it is also possible that the difference is the consequence of the surgical implantation procedure.

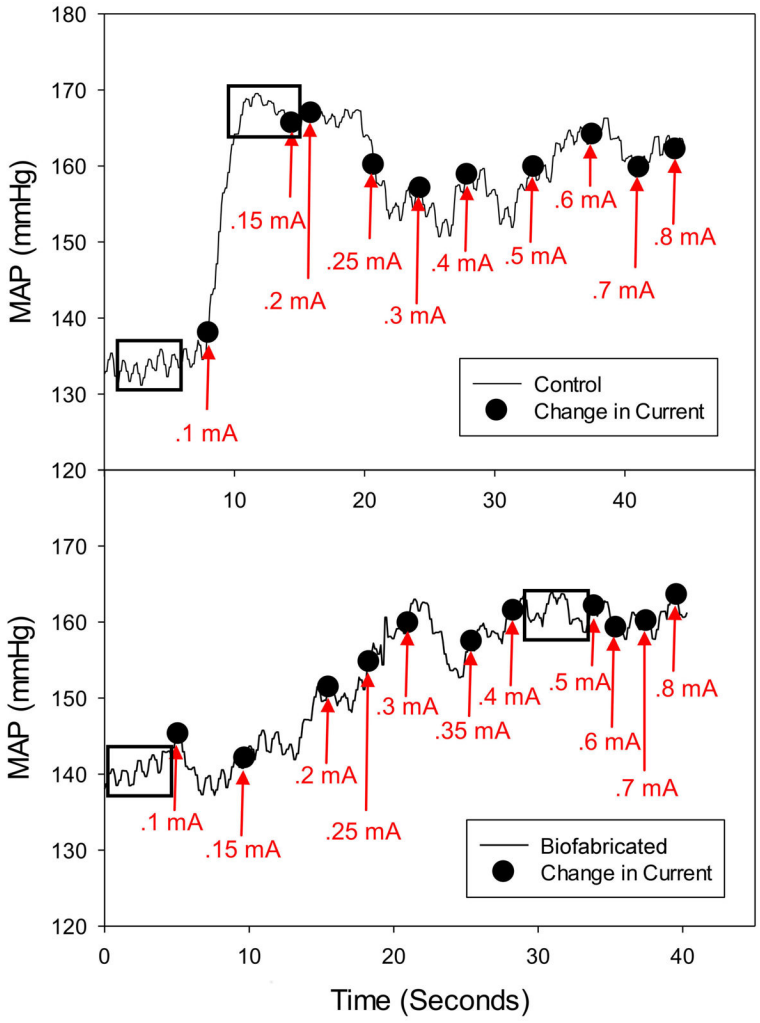

Figure 4.

Electrophysiology for sensory function recovery: somatic pressor reflex. The top and bottom panels refer respectively to the measurements of MAP in the control leg and the leg repaired with the biofabricated graft in the same animal. The solid black line represents the continuous raw record of MAP. The labeled black dots denote the approximate time of the current increase (manually marked using a foot pedal) with the associated value of current at that point in time. The base and maximum values of MAP were obtained by averaging values, respectively in the first and second boxed areas.

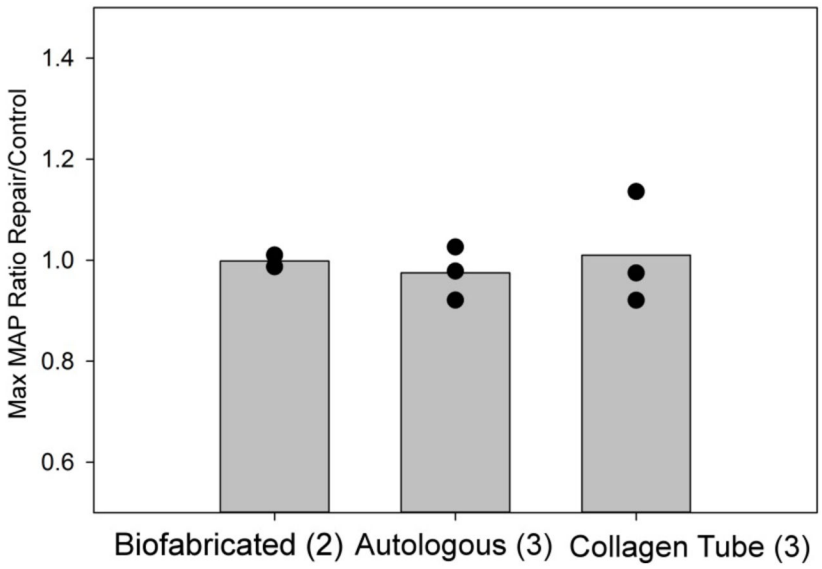

Figure 5.

Somatic Pressor Reflex: Maximum MAP response. The bar graphs show the average values of the ratios of maximum MAP in response to increasing sensory stimulation measured in the repair vs. control legs in the three types of grafts. Data points indicate the ratio of the maximum blood pressure in the repaired versus control legs for individual rats in that group (sample size is given in parenthesis).

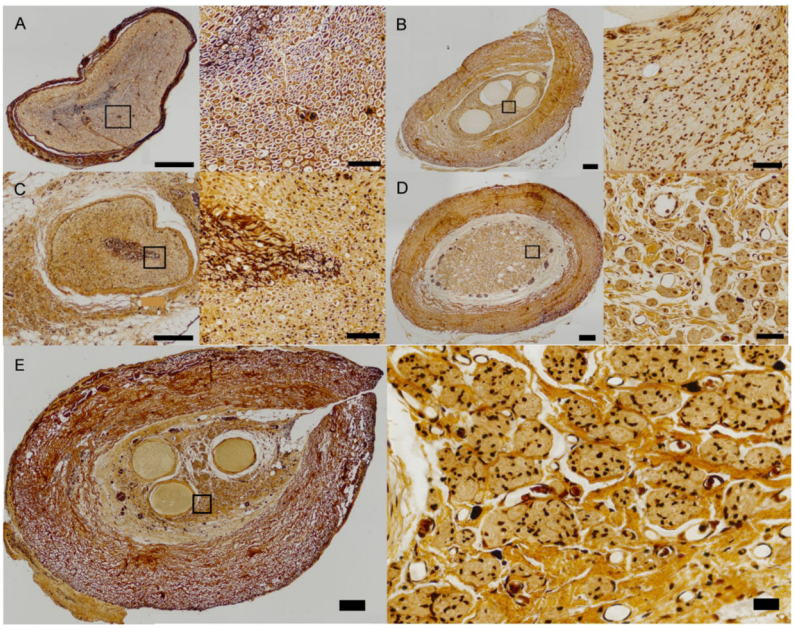

Figure 6.

Bielschowsky's staining of histological sections of the various types of grafts. A. Control (no surgery). B. Biofabricated graft. C. Autologous Graft. D. Collagen tube graft. In these images the left panels (showing the overall view of the cross sectional area) and right panels (enlarged view of the boxed regions on the left panels) correspond respectively to 200x and 600x magnifications. E. A more detailed view of one of the biofabricated grafts (left panel) and the axons across the boxed area (right panel). Axons in these images appear as black dots. All sections in these figures were taken at mid graft. Scale bars: 200 and 40 micron respectively for the left and right panels in all the images A–E.

Table 1

Latency to Peak data for CMAP.

	Control (ms)		Repair (ms)	
	Threshold	**5x Threshold**	**Threshold**	**5x Threshold**
Biofabricated Graft	1.97	1.56	4.30	2.20
	2.63	2.32	3.78	2.88
Mean±SEM	**2.30±0.33**	**1.94±0.38**	**4.04±0.26**	**2.54±0.34**
Autologous Graft	2.70	2.46	2.91	2.73
	2.31	1.97	3.28	2.41
	2.57	2.44	3.49	3.27
Mean±SEM	**2.53±0.11**	**2.29±0.16**	**3.23±0.17**	**2.80±0.25**
Collagen Tube Graft	2.44	2.07	4.06	3.74
	2.56	2.53	3.45	3.39
	3.01	2.70	4.08	2.80
Mean±SEM	**2.67±0.17**	**2.43±0.19**	**3.86±0.21**	**3.31±0.27**

Table 2

Maximum Blood Pressure Response.

	Control (mmHg)			Repair (mmHg)		
	Base MAP	**Max MAP**	**Change**	**Base MAP**	**Max MAP**	**Change**
Biofabricated Graft	130	163	34	132	165	33
	134	168	34	140	166	26
Mean±SEM	**132±2**	**165±3**	**34±0**	**136±4**	**165±1**	**29±4**
Autologous Graft	117	160	43	127	165	38
	154	176	22	141	172	31
	146	168	21	131	155	23
Mean±SEM	**139±11**	**168±5**	**29±7**	**133±4**	**164±5**	**31±4**
Collagen Tube Graft	143	169	26	120	156	36
	107	154	47	99	150	51
	132	148	16	141	168	27
Mean±SEM	**127±11**	**157±6**	**30±9**	**120±12**	**158±5**	**38±7**

Biofabrication. Author manuscript; available in PMC 2014 December 01.